Relations between statistically and mechanistically derived models: Analysis of a food-chain with complicated dynamics

Torsten Lindström
Division of Zoology, University of Oslo
Postboks 1050 Blindern, N-0316 Oslo, NORWAY
tel. +47-228 56186, fax. +47-228 54605
e-mail t.a.lindstrom@bio.uio.no

Abstract

In the qualitative part of this paper we present substantial evidence for that the dynamical patterns of food-chains predicted by Gragnani, De Feo and Rinaldi (Bull. Math. Biol., 1998) are robust with respect to discrete birth processes. Our theoretical study contains a rigorous proof of the discrete Hopf-bifurcation of the interior fixed point of the three dimensional system using the Schur-Cohn and the Routh-Hurwitz criteria. A detailed numerical investigation establishes the predicted patterns for non-equilibrium cases.

The statistical part is motivated by the increasing interest for using statistical methods outside their basic scope. Examples may include predicting number of species taking part in a given ecology or Lyapunov exponents from biological time-series. We fit both autoregressive models and multivariate adaptive regression splines (MARS) to data generated by our theoretical model and compare the statistical properties of the time series to our theoretical analysis.

Running head: Relations between statistically and mechanistically

Note: This report will be submitted for publication elsewhere

1 Introduction

The discussion about dynamical properties of food-chains is often traced back to Rosenzweig (1973). A detailed study of the properties of the equilibria of a continuous food-chain is found in his paper. Rosenzweig discussed mainly five equilibria in his paper, one corresponding to the origin, one corresponding to plants in the absence of other species, one corresponding to plant-herbivore interaction, and two corresponding to interaction between all species. If two equilibria of the last kind exist then at least one of them is unstable. Hence, four equilibria are usually important, one corresponding to each possible length of the food-chain. Furthermore, Rosenzweig noted that an invading carnivore either stabilizes or destabilizes plant-herbivore dynamics. Such stability properties have been related to food-chain length, cf. May (1971), May (1974), Pimm and Lawton (1977) and Pimm (1982).

The results by Freedman and Waltman (1977) open possibilities for relating the stabilizing properties of an invading carnivore to its unsaturatedness: An unsaturated carnivore keeps at least one interior equilibrium locally stable (if one exists). Stabilizing properties related to unsaturatedness in continuous systems are well known in the case of two-trophic level interaction, see Kuang and Freedman (1988). These stabilizing scenarios induced by invading carnivores were further studied with respect to enrichment by Oksanen, Fretwell, Arruda, and Niemelä (1981).

Possible destabilizing properties of saturated invading carnivores have been discussed by many authors recently, among them Gragnani, De Feo and Rinaldi (1998). They predicted that the dynamical complexity of a tritrophic food-chain first increases with respect to enrichment and then decreases until the carnivore goes extinct. Barren environments does not support a third trophic level at all (Chiu and Hsu (1998)) and if a system is supplied slightly above this level, stable coexistence is feasible. As the carrying capacity increases stable coexistence is not more allowed and a low-frequency cyclic coexistence occurs. The dynamical complexity still increases with enrichment and chaotic coexistence follows. The tea-cup attractor (Hastings and Powell (1991)) found here describes a transition between low- and high-frequency cycles. If the carrying capacity is still increased, these attractors become cut tea-cup attractor and resemble more and more simple cycles until a transition from chaos to cyclic behavior occurs. The cycles born in this transition have been called high-frequency cycles and resemble two-dimensional herbivore-vegetation cycles in that the carnivore density remain almost constant during

the oscillations. If the carrying is increased at this level the mean carnivore density goes down and if it is increased enough, the carnivore goes extinct.

Depending on the exact choice of the parameter values one or several phases of the above scenario can be short or omitted. The stability of the herbivore-vegetation system can also be regulated independently from carnivore-invasion. Thus, the boundary between the stabilizing and destabilizing scenarios is not sharp and certain mixes are allowed for. Klebanoff and Hastings (1994) also give examples for how multiple attractors (initial value dependent behavior) may evolve.

Models involving discrete birth-processes for interacting species have been introduced by Gyllenberg, Hanski, and Lindström (1996). In this paper a model for predator-prey interaction involving scramble competition at the lowest trophic level was introduced. Scramble-type competition is not the correct competition type for food-chains involving vegetation as their lowest trophic level, see Łomnicki (1988). An idea for including contest-type competition at the lowest trophic level in discrete models was given by Lindström (1999). In this paper we follow the approach taken in this paper, but because of the complexity of the model more restrictive assumptions are needed. Especially, we assume semelparity for all involved species which means that they reproduce once upon their life-time, cf. Cole (1954). Typical ecosystems possessing semelparity with non-overlapping generations at all trophic levels are those of terrestrial arthropods, cf. Borror, DeLong, and Triplehorn (1976). Further simplifications are that we approximate all expressions involving exponential integrals with elementary functions. These estimates are chosen with care and are valid for large parts of the phase- and parameter-space.

We continue with a detailed analytical investigation of the introduced model. Surprisingly, a rigorous proof of a discrete Hopf-bifurcation with respect to enrichment is obtained despite the formidable algebraic complexity in the stability analysis of most three dimensional discrete systems arising in applications. The Hopf-bifurcation is proven to be regular, ie it satisfies the transversality criterion with respect to enrichment and does not possess strong resonances.

In the numerical part we establish that the patterns predicted by Gragnani et. al. (1998) seem robust with respect to discrete birth processes. This result can be related to the fact that discrete and continuous systems seem comparable only when the same type of competition is appended to the lowest trophic level and scenarios related to the stabilizing properties of

unsaturatedness in continuous systems are neglected. Our study also reveals how possible violations of the assertions by Gragnani et. al. (1998) might arise.

Based on a study by Hassell, Lawton, and May (1976), Morris (1990) pointed out that problems exist when long-term qualitative behavior is predicted from models fitted to population data. The fitting techniques have later been developed, but the appropriateness of statistical models are still usually determined through some criterion related to "leave-one-out cross-validation". Therefore, we expect statistical models to be optimal with respect to one-step-ahead prediction and the available set of data. We remark that although relations between short-term prediction and chaos exist (Sugihara and May (1990)), they do not imply statistical models to be optimal in some other way. The debate concerning detection of density dependence from census data is related to this issue, too, cf. Nisbet, Blythe, Gurney, Metz, and Stokes (1989).

Nevertheless, an increasing interest for using statistical methods outside their scope of short-term prediction has been observed during the past decade. New attempts to determine the long-term qualitative behavior from census data (e. g. Turchin (1996)) have appeared and other examples exist, too. Stenseth, Bjørnstad, and Falck (1996) demonstrate the use of time-series methods for determining possible processes being important in ecological interaction and an attempt to predict the number of trophic levels taking part in a given ecology has been made by Stenseth, Falck, Bjørnstad, and Krebs (1997). The list could easily be extended and new methods assessing new quantities from census data are announced almost monthly. Concerning this era of techniques we feel that only the calculation of Lyapunov exponents from time-series data has received a part of the relevant criticism, cf. Vibe and Vesin (1996).

In the statistical part (Sections 5-6) we fit statistically motivated models to the data generated by our discrete model. The relationship between statistical and mechanistical models is not simple and we think that there is a need for knowing what to expect when models are fitted to data. We address some of the questions related to the new quantities announced predictable from census data. The coefficients and dimensions of autoregressive models are evaluated first and then multivariate adaptive regression splines are fitted to data using lagged variables as surrogates for unknown variables, cf. Lewis and Stevens (1991).

2 A discrete model for a food-chain

In this section we build up our main model. A number of authors have investigated discrete food-chains possessing scramble competition at the lowest trophic level. These models possess possibilities for two major scenarios: the invasion of higher trophic levels may both stabilize or destabilize the dynamics at lower trophic levels, see e. g. Beddington and Hammond (1977). The same holds for continuous food-chains, but here the stabilizing scenario is related to the level of unsaturatedness of the invading higher trophic level, cf. Section 1. The competition-type assumed for continuous food-chains have usually been of contest-type since other competition types would require taking into account the structure of the population at the lowest trophic level, cf. Gyllenberg, Hanski, and Lindström (1997).

In order to make discrete models comparable to continuous ones it is necessary to assume a competition form which is close to the commonly assumed logistic competition of the continuous models. Doing so we obtain a discrete food-chain which differs from the continuous food-chains only in that discrete birth processes are assumed. Also other reasons exist: neglecting competition would result in models as unstable as the Nicholson-Bailey (1935) model, cf. May (1973). In comparison, the Lotka (1925) and Volterra (1926) model possesses bounded oscillations and we take this as a preliminary confirmation that unsaturatedness has a stabilizing impact on continuous systems which is absent in discrete systems.

The inclusion of contest competition at the lowest trophic level of a discrete model is not a straightforward process. Contest-competition usually operates over longer parts of the season than scramble competition. Thus, we must take into account that some of the individuals taking part in the competition are removed by other processes, in our case predation. This puts limits on how complicated models we can build up and is one reason for why continuous modeling has been preferred for modeling purposes, cf. Metz and Diekmann (1984).

We assume that both the carnivore and the herbivore are unsaturated and divide the vegetation into plants receiving enough light for reproduction in the beginning of the next season and plants not doing so. In the beginning of the season all new-born plants have the potential to reproduce, but as the season goes on more of them are excluded. For simplicity, we assume that this exclusion process is governed by the death processes of the logistic equation. We also assume that vegetation excluded from reproduction remains equally

exposed to herbivores as vegetation with potential to reproduce. Following Lindström (1999) we obtain the following equations for the death processes

$$\begin{aligned}
\dot{x}_R &= -kx_R^2 - ax_R y, & x_R(0) &= x_0 \\
\dot{x}_F &= +kx_R^2 - ax_F y, & x_F(0) &= 0 \\
\dot{y} &= -byz, & y(0) &= y_0 \\
\dot{z} &= 0, & z(0) &= z_0.
\end{aligned}$$

We have assumed no natural death since we are going to assume semelparity and this limits lifetime of the individuals. Put $x = x_R + x_F$ so that $\dot{x} = -axy$. We solve the above system of equations and get

$$\begin{aligned}
x(t) &= x_0 \exp\left(-ay_0 t \cdot \frac{1-\exp(-bz_0 t)}{bz_0 t}\right), \\
y(t) &= y_0 \exp(-bz_0 t), \\
z(t) &= z_0.
\end{aligned}$$

These equations denote the individuals still alive at the end of the season. In the case of plants, some of them are able to reproduce. They are given by

$$x_R(t) = \frac{x_0 \exp\left(-ay_0 t \cdot \frac{1-\exp(-bz_0 t)}{bz_0 t}\right)}{1 + \frac{kx_0 t}{bz_0 t}\exp\left(-\frac{ay_0 t}{bz_0 t}\right)\left(\mathrm{Ei}\left(\frac{ay_0 t}{bz_0 t}\right) - \mathrm{Ei}\left(\frac{ay_0 t}{bz_0 t}\exp(-bz_0 t)\right)\right)},$$

where

$$\mathrm{Ei}(x) = \int_{-\infty}^{x} \frac{\exp(\xi)}{\xi} d\xi.$$

is to be evaluated as a Cauchy principal value.

Now assume that the reproducing plants x_R reproduce with a mean of M_0 offspring at the time instant T. Simultaneously, we assume that a fraction of the consumed vegetation and herbivore biomass is converted into herbivore and carnivore biomass, respectively. We take into account that the whole consumption does not correspond to herbivores or carnivores alive at the end of the season. We get

$$\begin{aligned}
x(T) &= \frac{M_0 x_0 \exp\left(-ay_0 T \cdot \frac{1-\exp(-bz_0 T)}{bz_0 T}\right)}{1 + \frac{kx_0 T}{bz_0 T}\exp\left(-\frac{ay_0 T}{bz_0 T}\right)\left(\mathrm{Ei}\left(\frac{ay_0 T}{bz_0 T}\right) - \mathrm{Ei}\left(\frac{ay_0 T}{bz_0 T}\exp(-bz_0 T)\right)\right)}, \\
y(T) &= m_1 x_0 a y_0 T \cdot \exp(-bz_0 T) \cdot \frac{1 - \exp\left(-ay_0 T \cdot \frac{1-\exp(-bz_0 T)}{bz_0 T}\right)}{ay_0 T},
\end{aligned}$$

$$z(T) = m_2 y_0 b z_0 T \cdot \frac{1-\exp(-bz_0T)}{bz_0T},$$

if we assume semelparity at all trophic levels. Now put

$$\begin{aligned} X &= kx_0T, \\ Z &= bz_0T, \\ M_1 &= m_1a/k, \\ M_2 &= m_2b/a, \\ \kappa(\gamma) &= (1-\exp(-\gamma))/\gamma, \\ H(\alpha,\rho) &= -\exp(-\rho)(\mathrm{Ei}(\rho)-\mathrm{Ei}(\alpha\rho))/\log\alpha, \\ U &= ay_0T\kappa(bz_0T). \end{aligned}$$

We can assume $T=1$ without loss of generality and get

$$\begin{aligned} X_{t+1} &= \frac{M_0X_t\exp(-U_t)}{1+X_tH\left(\exp(-Z_t),\frac{U_t}{1-\exp(-Z_t)}\right)}, \\ U_{t+1} &= M_1X_tU_t\exp(-Z_t)\kappa(U_t)\cdot\kappa\left(M_2U_tZ_t\right), \\ Z_{t+1} &= M_2U_tZ_t. \end{aligned} \tag{1}$$

We remark that the introduction of the new variable U left our subsequent statistical analysis (Sections 5-6) largely unchanged. It is therefore convenient to represent the herbivores by this variable throughout the paper. It follows from Lindström (1999), Proposition 3.1(f) that the rather complicated function H can be estimated by

$$H(\exp(-Z),U/(1-\exp(-Z))) \approx \max(\exp(-U),\kappa(Z)\kappa(U)).$$

and the system to be studied takes the form

$$\begin{aligned} X_{t+1} &= \frac{M_0X_t\exp(-U_t)}{1+X_t\max(\exp(-U_t),\kappa(Z_t)\kappa(U_t))} \\ U_{t+1} &= M_1X_tU_t\exp(-Z_t)\kappa(U_t)\cdot\kappa\left(M_2U_tZ_t\right) \\ Z_{t+1} &= M_2U_tZ_t. \end{aligned} \tag{2}$$

We verified the above estimate also numerically for the parameters values used in our numerical analysis and only minor differences were detected, see in particular Remark (b) after Theorem 3.4. Since the model (1) remain more complicated than (2) also numerically we have replaced the model (1) with (2) throughout the rest of the paper for simplicity.

We begin with the following basic lemma.

Lemma 2.1. *Solutions of* (2) *remain positive and bounded.*

Proof. Positiveness follows directly from the equations. From the equation for X_{t+1} it follows that succeeding values of X_t are bounded by M_0. From the equation for U_{t+1} we get

$$U_{t+2} < \frac{U_{t+2}}{\kappa(Z_{t+2})} < M_1 M_0.$$

From the last equation we get

$$Z_{t+3} < M_2 \frac{U_{t+2}}{\kappa(Z_{t+2})} Z_{t+2} \kappa(Z_{t+2}) < M_2 M_1 M_0,$$

in the next iteration. Thus, all solutions starting in the positive cone enter the box $0 < X < M_0$, $0 < U < M_0 M_1$, $0 < Z < M_0 M_1 M_2$ within three iterations. □

The system (2) admits at most four equilibria, one corresponding to each possible length of the food-chain. We label them as $(0, 0, 0)$, $(M_0 - 1, 0, 0)$, $(X_\star, U_\star, 0)$, and $(\hat{X}, \hat{U}, \hat{Z})$. The uniqueness $(\hat{X}, \hat{U}, \hat{Z})$ follows from the fact that the right-hand side of

$$1 = M_1 \frac{M_0 \exp(-1/M_2) - 1}{\max(\exp(-1/M_2)\kappa(1/M_2)\kappa(Z))} \kappa(1/M_2) \exp(-Z)\kappa(Z)$$

is a continuous and strictly decreasing function of Z. Since the XZ-plane and the UZ-plane do not introduce any new asymptotic behavior, the persistence criteria for vegetation and herbivores remain unchanged with respect to the herbivore-vegetation system. That is, if $M_0 > 1$ and $M_0 > (M_1 + 1)/M_1$ then vegetation and herbivores persist, respectively.

The following lemma shows together with the dynamical properties of the herbivore-vegetation system that persistence criteria for the carnivore must be considered separately and can be a difficult to formulate. The proof of the lemma follows from the equation for Z_{t+1} in (2).

Lemma 2.2. *If*

$$\lim_{n\to\infty} \sqrt[n]{\prod_{i=0}^{n-1} U_i} < \frac{1}{M_2}. \tag{3}$$

then (2) *predicts* $\lim_{n\to\infty} Z_n = 0$.

Lemma 2.2 states together with Lemma 2.1 that the asymptotic geometric mean of the herbivore population must equal $1/M_2$, otherwise the carnivores go extinct. Since asymptotic behavior of the herbivore-vegetation system normally includes multiple attractors (cf. Aronson, Chory, Hall, and McGehee (1982)) it can be a delicate matter to find out weather all possible coexisting attractors have the same properties with respect to (3). As long as this question does not have answer there might be one attractor in the herbivore-vegetation plane allowing local carnivore invasion together with one giving rise to local extinction. However, according to our numerical analysis it seems that we are likely to observe is an interval with respect to M_0 which allows carnivore invasion and persistence. This can be explained in two ways: either possible coexisting attractors possess asymptotic geometric means which remain close to each other or carnivore invasion occurs usually for parameter values not allowing multiple attractors in the herbivore-vegetation system.

3 Equilibria

As concluded in Section 2, (2) possesses at most four equilibria which we referred to as $(0,0,0)$, $(M_0-1,0,0)$, $(X_\star,U_\star,0)$, and $(\hat{X},\hat{U},\hat{Z})$. The Jacobian of (2) evaluated at the first two of these equilibria allows triangular or diagonal representation and thus, the stability properties of these equilibria are simple. The coordinates of the third equilibrium are given by

$$(X_\star,U_\star,0)=\left(\frac{M_0\log\left(\frac{M_1M_0}{1+M_1}\right)}{(M_0-1)M_1-1},\log\left(\frac{M_1M_0}{1+M_1}\right),0\right). \tag{4}$$

The second coordinate of (4) and Lemma 2.2 give:

Corollary 3.1. *The carnivores go extinct near* $(X_\star,U_\star,0)$ *if*

$$M_0<\exp(1/M_2)(M_1+1)/M_1. \tag{5}$$

The carnivores invade near $(X_\star,U_\star,0)$ *if the converse inequality holds.*

On the basis of the above corollary we know all stability properties of (4) which are related to motion outside the invariant XU-plane. We shall therefore restrict the further stability analysis of (4) to that plane. The

system (2) restricted accordingly takes the form

$$\begin{aligned} X_{t+1} &= \frac{M_0 X_t \exp(-U_t)}{1 + X_t \kappa(U_t)}, \\ U_{t+1} &= M_1 X_t (1 - \exp(-U_t)). \end{aligned} \tag{6}$$

The next theorem follows using the ideas of Lindström (1999). Its proof is included for convenience.

Theorem 3.2. *The equilibrium* (4) *is locally stable in the invariant XU-plane when*

$$\frac{M_0 \log \frac{M_1 M_0}{1+M_1}}{(M_0 - 1)M_1 - 1} < \frac{1}{M_1} \cdot \frac{M_1 + 2}{M_1 + 1} \tag{7}$$

and unstable when the converse inequality holds. If equality holds in (7) *and* M_0 *is used as bifurcation parameter, then* (4) *undergoes a Hopf-bifurcation.*

Proof. Note that $\kappa'(U) = (\exp(-U) - \kappa(U))/U$. The Jacobian of the system (6) at $(X_\star, U_\star)$ is given by

$$J_\star(X_\star, U_\star) = \begin{pmatrix} \frac{M_1}{M_1+1} & -\frac{X_\star}{U_\star}\frac{M_1 U_\star + M_1 X_\star - 1}{M_1+1} \\ U_\star / X_\star & M_1 X_\star - U_\star \end{pmatrix} \tag{8}$$

We require

$$-1 + |\mathrm{Tr} J_\star(X_\star, U_\star)| - \det J_\star(X_\star, U_\star) < 0, \tag{9}$$

$$-1 + \det J_\star(X_\star, U_\star) < 0 \tag{10}$$

for local stability and get

$$\begin{aligned} \mathrm{Tr} J_\star(X_\star, U_\star) &= \frac{M_1}{M_1 + 1} + M_1 X_\star - U_\star \\ \det J_\star(X_\star, U_\star) &= \frac{M_1^2 X_\star + M_1 X_\star - 1}{M_1 + 1} \end{aligned}$$

Since $U_\star < M_1 X_\star$, expression (9) is equivalent to $-U_\star < 0$ which is identically true. It follows from the relationship between roots and coefficients of a quadratic equation that if $(X_\star, U_\star)$ undergoes a bifurcation, then $J_\star(X_\star, U_\star)$ must possess complex eigenvalues with positive real parts. Thus, strong resonances connected to a discrete Hopf-bifurcation are excluded.

We proceed to (10). It states that $(X_\star, U_\star)$ is stable if,

$$X_\star < \frac{1}{M_1} \cdot \frac{M_1 + 2}{M_1 + 1}, \tag{11}$$

and unstable, if the converse inequality holds. Since $X_\star$ is a strictly increasing function of M_0, the transversality condition holds using M_0 as bifurcation parameter. It follows that the Hopf-bifurcation occurs for exactly one value of M_0 as it increases. Strong resonances were earlier excluded and substitution of (4) in (11) gives the stability criterion (7). □

We proceed with the fourth equilibrium $(\hat{X}, \hat{U}, \hat{Z})$. As long as

$$\max(\exp(-\hat{U}), \kappa(\hat{U})\kappa(\hat{Z})) = \kappa(\hat{U})\kappa(\hat{Z}) \tag{12}$$

it is given by

$$\left(\frac{M_0 e^{-1/M_2} - 1}{\kappa\left(\frac{1}{M_2}\right) \kappa\left(\log M_1 \left(M_0 e^{-\frac{1}{M_2}} - 1\right)\right)}, \frac{1}{M_2}, \log M_1 \left(M_0 e^{-\frac{1}{M_2}} - 1\right) \right). \tag{13}$$

Our numerical analysis (Section 4) reveals that (13) yields the relevant coordinates for $(\hat{X}, \hat{U}, \hat{Z})$ as long as it remains locally stable for most realistic values of M_0, M_1, and M_2. The following lemma gives some preliminary estimates needed for the proof of the next theorem. The lemma follows from the equation for U_{t+1} in (2) and the definition of κ.

Lemma 3.3. *We have:*

(a) $\max(1, \hat{U}) < \frac{1}{\kappa(\hat{U})} = M_1 \hat{X} \exp(-\hat{Z})\kappa(\hat{Z})$,

(b) $-\frac{\kappa'(\hat{Z})}{\kappa(\hat{Z})} = \frac{\kappa(\hat{Z}) - \exp(-\hat{Z})}{1 - \exp(-\hat{Z})} < \kappa(\hat{Z})$.

Theorem 3.4. *Let* $\mathcal{M} = M_1 \exp(-\hat{Z})$ *and* $\mathcal{K} = -\kappa'(\hat{Z})/\kappa(\hat{Z})$. *Assume* (12) *and*

$$M_1 > \min\left(1 - \exp\left(-\frac{1}{M_2}\right), \kappa\left(\frac{1}{M_2}\right)\right). \tag{14}$$

The equilibrium (13) *is locally stable if*

$$\mathcal{M}\hat{X}\kappa(\hat{Z}) < \frac{2 + \mathcal{M} - \mathcal{M}\hat{Z} - \mathcal{K}\hat{Z}}{1 + \mathcal{M}} - \frac{\hat{Z}}{\hat{U}(1 + \mathcal{M}) + \mathcal{K}\hat{Z}(2 + \mathcal{M}) + \mathcal{M}\hat{Z}} \tag{15}$$

and unstable when the converse inequality holds. If equality in (15) *holds and* M_0 *is used as bifurcation parameter, then* (13) *undergoes a Hopf-bifurcation.*

Remarks

(a) Since a regular Hopf-bifurcation occurs, we expect periods larger than four to be observed. This is a first indication that herbivore-vegetation cycles cannot be distinguished from carnivore-herbivore cycles by measuring periods close to a bifurcation, cf. also Theorem 3.2. Section 4 provides further evidence of this fact.

(b) For some parameter values satisfying (12), (14), and (15) we detected also quasi- or high-periodic behavior, ie attractors involving alternatives to stable dynamics. One example is $M_0 = 3.052$, $M_1 = .9355$, and $M_2 = 4.0$. We did not observe multiple attractors for the smooth system (1) at the corresponding parameter values so this phenomenon might have been introduced by our approximation (2). The parameter range possessing this phenomenon was usually narrow and hard to detect.

(c) Condition (14) was needed in our proof to exclude strong resonances. It can probably be removed from the theorem but we did not found this condition too restrictive, either.

(d) We conjecture that the implication (15) $\Rightarrow$ (7) holds but it seems difficult to construct a proof of this fact for the whole parameter range (12) and (14). Numerical experiments indicated something similar to hold also outside (12) and (14). Remarkable ecological consequences follow if this implication remains true. The result is reminiscent of those obtained by May (1971) and excludes the possibility for food-web complexity induced stability in (2).

Proof. The Jacobian of (2) evaluated at (13) assumed (12) is given by

$$\begin{pmatrix} \frac{\mathcal{M}}{\mathcal{M}+1} & -\frac{\hat{X}}{\hat{U}} \cdot \frac{\mathcal{M}\hat{U}+\mathcal{M}\hat{X}\kappa(\hat{Z})-1}{\mathcal{M}+1} & \frac{\hat{X}\mathcal{K}}{\mathcal{M}+1} \\ \hat{U}/\hat{X} & \mathcal{M}\hat{X}\kappa(\hat{Z}) - \hat{U} - \mathcal{K}\hat{Z} & -\hat{U} - \hat{U}\mathcal{K} \\ 0 & \hat{Z}/\hat{U} & 1 \end{pmatrix} \tag{16}$$

The characteristic equation of (16) takes the form

$$\lambda^3 + \lambda^2 \frac{-1 + \hat{U} - \kappa(Z)\mathcal{M}^2\hat{X} + \mathcal{K}\hat{Z} - 2\mathcal{M} + \hat{U}\mathcal{M} - \kappa(\hat{Z})\mathcal{M}\hat{X} + \mathcal{M}\mathcal{K}\hat{Z}}{1+\mathcal{M}} +$$

$$\lambda\frac{-1-\hat{U}+2\kappa(\hat{Z})\mathcal{M}^2\hat{X}+\hat{Z}+\mathcal{M}-\mathcal{M}\hat{U}+2\kappa(Z)\mathcal{M}\hat{X}+\mathcal{M}\hat{Z}-\mathcal{M}\mathcal{K}\hat{Z}}{1+\mathcal{M}}+$$
$$\frac{1-\kappa(\hat{Z})\mathcal{M}\hat{X}-\kappa(\hat{Z})\mathcal{M}^2\hat{X}-\mathcal{K}\hat{Z}-\mathcal{M}\hat{Z}}{1+\mathcal{M}}=0$$

The Schur-Cohn criteria, see e.g. Schur (1917,1918), Cohn (1922), Jury (1964), Marden (1966), and May (1974) for the cubic equation

$$\lambda^3+\alpha\lambda^2+\beta\lambda+\gamma=0$$

are given by

$$1-\gamma^2 > |\alpha\gamma-\beta| \quad (17)$$
$$|1+\beta| > |\alpha+\gamma| \quad (18)$$

Note that Lemma 3.3 yields

$$\gamma<0, \quad (19)$$
$$\alpha<0. \quad (20)$$

Condition (18) can be stated as

$$|2\kappa(\hat{Z})\mathcal{M}^2\hat{X}-\mathcal{M}\hat{U}+2\kappa(\hat{Z})\mathcal{M}\hat{X}-\hat{U}+\mathcal{M}\hat{Z}+2\mathcal{M}-\mathcal{K}\mathcal{M}\hat{Z}+\hat{Z}| >$$
$$|-2\kappa(\hat{Z})\mathcal{M}^2\hat{X}+\mathcal{M}\hat{U}-2\kappa(\hat{Z})\mathcal{M}\hat{X}+\hat{U}-\mathcal{M}\hat{Z}-2\mathcal{M}+\mathcal{K}\mathcal{M}\hat{Z}|.$$

From Lemma 3.3 we get

$$2\kappa(\hat{Z})\mathcal{M}^2\hat{X}-\mathcal{M}\hat{U}+2\kappa(\hat{Z})\mathcal{M}\hat{X}-\hat{U}+\mathcal{M}\hat{Z}+2\mathcal{M}-\mathcal{K}\mathcal{M}\hat{Z}>0. \quad (21)$$

Thus, (18) holds identically. It follows from the relationship between roots and coefficients for a cubic equation that a pair of complex eigenvalues must be involved in any exchange of stability of the fixed point (13).

Now consider (17). By (19), we require $-1<\gamma<0$ for stability. Depending on the sign inside the absolute sign, (17) assumes one of the forms

$$1+\beta>\gamma(\gamma+\alpha), \quad (22)$$
$$1-\beta>\gamma(\gamma-\alpha). \quad (23)$$

Superfluousness of (22) follows from (18), (19), and (21). Accordingly, possible bifurcations satisfy

$$1-\beta=\gamma(\gamma-\alpha). \quad (24)$$

Let γ_i, $i = 1, 2$ be the two solutions of (24). Lemma 3.3 gives

$$-2 - \hat{U} + 2\kappa(\hat{Z})\mathcal{M}^2\hat{X} + \hat{Z} - \mathcal{M}\hat{U} + 2\kappa(Z)\mathcal{M}\hat{X} + \mathcal{M}(1-\mathcal{K})\hat{Z} \quad > \quad (25)$$

$$-\min(1, \hat{U}) + \frac{\mathcal{M}}{\kappa(\hat{U})} + \hat{Z} + \mathcal{M}(1-\mathcal{K})\hat{Z} \qquad (26)$$

which implies $\beta > 1$ for $M_1 \geq 1$ or $\hat{Z} \geq 1$. If $M_1 < 1$ and $\hat{Z} < 1$ then (26) increases with $\hat{Z}$ and $\beta > 1$ follows from (14). It follows from (20) and (24) that $\alpha\beta < \alpha < \gamma_1 \leq \gamma_2 < 0$. Thus, the characteristic equation of (16) possesses the Hurwitz determinant sequence $\{1, \alpha, \alpha(\alpha\beta - \gamma), \gamma\}$, cf. Marden (1966, p 180), which has three sign-changes. This implies the real part of all characteristic roots to be positive. The bifurcation is a Hopf-bifurcation and strong resonances are excluded. The stability criterion (15) follows from direct substitution in (23).

We continue by checking the transversality condition with respect to M_0. The left-hand side of (15) is constant with respect to M_0 and greater than one (Lemma 3.3). The second term of the right-hand side is strictly decreasing (consider its reciprocal). We write the first term as

$$\frac{2 + \mathcal{M} - \mathcal{M}\hat{Z} - \mathcal{K}\hat{Z}}{1 + \mathcal{M}} = 1 + \frac{\exp(-\hat{Z})}{\kappa(\hat{Z})}\left(1 - \frac{M_1}{1 + \mathcal{M}}\right)$$

The above expression is strictly decreasing as long as it remains greater than one. It tends to one as $\hat{Z}$ tends to infinity. It follows that equality occurs in (15) for a unique value of $\hat{Z}$. When equality occurs, the right-hand side of (15) has strictly negative derivative with respect to $\hat{Z}$. Since $\hat{Z}$ is an increasing function of M_0 it follows from the chain rule that the right-hand side of (15) decreases with respect to M_0 when equality occurs. Thus, the transversality criterion of the Hopf-bifurcation theorem holds. □

4 Numerical investigation of the food-chain model

We complete the above theoretical study with a numerical study. The results for $M_1 = 1.$ and $M_2 = 4.$ appear quite typical and can be found in Figure 1. These parameter values satisfy (12) and (14) as long as $(\hat{X}, \hat{U}, \hat{Z})$ remains locally stable. The dynamics of the complete chain (2) is represented by a

solid line whereas the corresponding dynamics of the carnivore-free system (6) is represented with a dotted line. The vertical dotted lines denote different regions of the parameter space including those predicted by Lemma 2.2, Corollary 3.1, Theorem 3.2, and Theorem 3.4.

Region A denotes small values of the bifurcation parameter M_0. For such values the vegetation persists and is stable. Region B represents persistent and stable vegetation and herbivore populations. In region C stable coexistence between all species is permitted. Between C and D the Hopf-bifurcation predicted by Theorem 3.4 occurs and D represent non-chaotic oscillatory coexistence. Figure 1(a) confirms that the amplitude of the oscillations grows as a parabola in region D and Figure 1(c) shows a dominating period (period corresponding the maximum of the Fourier-transform of the solution) larger than four, as predicted by Remark (a) after Theorem 3.4. At the end of region C a narrow region possessing alternative quasi- or high-periodic attractors may exist, cf. Remark (b) after Theorem 3.4. These attractors had approximately the same dominating periods as the attractors observed in the beginning of region D.

A complicated transition to chaos is predicted to occur after the Hopf-bifurcation, cf. Aronson et. al. (1982). This transition involves quasiperiodic and periodic solutions. The pattern is confirmed by Figure 1(b) which gives the periods of the solutions (if any below 1024 was found). Figure 1(d) gives the Lyapunov exponent which remains close to zero throughout region D.

The transition to chaos is complete in region E but we note simultaneously that the solutions interact to a large extent with the fixed point dynamics of the carnivore-free system (6). It seems therefore unclear to what extent the transition to chaos at this stage in general occurs due to such interaction, cf. Gragnani et. al. (1998) or can be reduced to occur in some two-dimensional invariant manifold, cf. Aronson et. al. (1982). When interaction occurs, a torus-like attractor (Ives and Jansen (1998)) describes the motion. The Hopf-bifurcation predicted by Theorem 3.2 occurs between regions E and F. The carnivore-herbivore oscillations start to interact with unstable herbivore-vegetation dynamics. A tea-cup like attractor (Hastings and Powell (1991)) is formed and the dynamics is described by a mixture of low-frequency (carnivore-herbivore) oscillations and high-frequency (herbivore-vegetation) oscillations.

Note that despite the high-frequency character of the herbivore-vegetation and the low-frequency character of the carnivore-herbivore cycles, these two kinds of cycles are indistinguishable from each other with respect to their pe-

riods when not interfering with each other. That is, the oscillations emerging from the interior Hopf-bifurcation of (2) between C and D and the oscillations emerging from the Hopf-bifurcation of (6) between E and F possess almost the same dominating periods as already indicated by Remark (a) after Theorem 3.4. Therefore we do not expect pure carnivore-herbivore cycles (region D) to differ essentially from pure herbivore-vegetation cycles (regions H-I).

This scenario is most visible in Figure 1(c) although we do not expect properties like dominating periods to be invariant with respect to one-to-one coordinate transformations here. In region F the vegetation time-series (solid line) often take dominating periods almost equal to those observed in (6) (dotted line). In fact, the vegetation time-series follow the patterns of two-dimensional high-frequency (herbivore-vegetation) oscillations for long-periods and are for short periods only affected by high carnivore densities. The same does not hold for the carnivore time-series (dashed line) and low-frequency behavior dominates the Fourier-spectrum.

The amplitude of the oscillations, Figure 1(a), reaches its maximum between F and G and here carnivore oscillations are the most dominating. In region G the high-frequency (herbivore-vegetation) oscillations dominate more and more and in region H the carnivore-induced chaos disappears, cf. Figure 1(d). We get herbivore-vegetation cycles with co-oscillating carnivores. Lemma 2.2 excludes carnivores in region I. For parameter-values far beyond those interesting in the three-dimensional case and moderate values of M_2, the two-dimensional oscillations undergo a transition to chaos, cf. Aronson et. al. (1982).

Figure 2 illustrates the above patterns in the three-dimensional parameter space (M_0, M_1, M_2). If $M_2 = 0$ the system (2) is fully described by the two-parameter system (6) (Lemma 2.2). Figure 2(a) gives a description of (6) in the parameter plane (M_0, M_1). Herbivore extinction is indicated by green dots, locally stable coexistence by black dots, low-periodic solutions by yellow dots, high-periodic solutions by light blue dots, and quasi-periodic- or bifurcating solutions by blue dots. Finally, red dots denote the chaotic solutions.

When $M_2 \neq 0$ certain areas of the parameter plane in Figure 2(a) are affected by carnivore invasion. The lower bound of these areas are determined by the equality corresponding to (5). A white line in Figure 2(a) demonstrates this boundary in the cases $M_2 = 3.$ (solid) and $M_2 = 4.$ (dashed). The areas above these boundaries are partially affected by carnivore invasion

and the areas affected have been plotted in Figure 2(b) and Figure 2(c) for $M_2 = 3.$ and $M_2 = 4.$, respectively.

As a reference, the boundary between the locally stable and oscillating solutions in Figure 2(a) has been denoted by a black line in Figures 2(b)-(c). This line corresponds to the bifurcation predicted by Theorem 3.2 and to substantially higher values of M_0 than the transition between locally stable and oscillatory solutions predicted by Figures 2(b)-(c). This is in concordance with our expectation that the implication (15) $\Rightarrow$ (7) should be valid in a wide sense and shows that carnivore-invasion is expected to destabilize the dynamics of (2), cf Remark (d) after Theorem 3.4.

To check the applicability range of Theorem 3.4 we also plotted a purple line in Figures 2(b)-(c). It denotes maximal M_0 for which (12) holds. We see that Theorem 3.4 contains enough information to describe the transition from locally stable to oscillatory dynamics when $M_2 = 3.$ for all values of M_1 used in Figure 2(b). The applicability range of Theorem 3.4 is not that clear in the case $M_2 = 4.$ (Figure 2(c)). We enlarged the critical parts of this case in Figure 2(d). We also denoted the transition between locally stable and oscillating dynamics as predicted by (15) with a dashed purple line. The dashed line intersects the solid line approximately at $(M_0, M_1) = (3.1056, .91501)$. Thus, the transition from locally stable to oscillating dynamics with enrichment is no longer described by Theorem 3.4 as $M_1 < .91501$ when $M_2 = 4.0$.

The patterns involving interaction between low- and high-frequency cycles suggest further analysis of the relationship between yield and dynamic behavior (Gragnani et. al. (1998)). Figure 3(a) shows how the mean carnivore abundance responds to enrichment in our discrete food-chain. Actually, it has two local maxima and one local minimum. The first local maximum corresponds to the Hopf-bifurcation between regions C and D. This is the highest level of enrichment that gives rise to a stable carnivore population. The local minimum corresponds to the boundary between F and G, and we concluded earlier that this value corresponds to the most unstable carnivore population. A second local maximum occurs when the low-frequency oscillations disappear together with the chaos at the boundary between G and H. Region H denotes a new regime with quite stable carnivore populations. Thus, the boundary between chaos and non-chaos has the optimizing properties described by Gragnani et. al. (1998) also in this discrete system.

Simultaneously, our result yields possibilities for seeing under what conditions this result might be violated. If the herbivore-vegetation cycles are chaotic, there will not be a transition from chaos to periodic or quasi-periodic

behavior as carnivore-herbivore oscillations turn over to herbivore-vegetation oscillations. According to our experiments very high values of M_2 must be used to demonstrate such violations. The transition from stable to oscillating dynamics would not be described by Theorem 3.4 in this case but it can be a delicate matter for a subsequent study. Since the transition to chaos of (6) normally includes multiple attractors, the region is interesting with respect to carnivore invasion, too, cf. our comments regarding Lemma 2.2.

5 Autoregressive modeling of the food-chain

We added normally distributed noise on a logarithmic scale to (2) as described by Cushing, Dennis, Desharnais and Costantino (1996) and Ives and Jansen (1998). Such a stochastic version of (2) incorporates environmental variability and takes the form

$$\begin{aligned} X_{t+1} &= \frac{M_0 \exp(\varphi_{1t}) X_t \exp(-U_t)}{1 + X_t \max(\exp(-U_t), \kappa(Z_t)\kappa(U_t))}, \\ U_{t+1} &= M_1 \exp(\varphi_{2t}) X_t U_t \exp(-Z_t)\kappa(U_t) \cdot \kappa\left(M_2 U_t Z_t\right), \\ Z_{t+1} &= M_2 \exp(\varphi_{3t}) U_t Z_t. \end{aligned} \tag{27}$$

Here $(\varphi_{1t}, \varphi_{2t}, \varphi_{3t})$ is a random vector assumed to have trivariate normal distribution and covariances close to zero. In region A the standard deviations of φ_{it}, $i = 1, 2, 3$ were .1, in regions B and I they were $.1/\sqrt{2}$, and in regions C-H they were $.1/\sqrt{3}$. Thus, in the relevant (logarithmic) phase-space we perturbed the location by a mean distance of .1 in a randomly chosen direction after each iteration.

To avoid transient dynamics we iterated the models a substantial amount of times before three time-series (one for vegetation, herbivores, and carnivores, respectively) of length 256 were randomly chosen for each parameter value. In several cases statistical methods have been applied to ecological time-series considerably shorter than that, see e. g. Stenseth, Bjørnstad, and Saitoh (1996) and Stenseth et. al. (1996)[47].

The coefficients a_{11}, a_{21}, a_{22}, a_{31}, a_{32}, a_{33} of the three different autoregressive models

$$\chi_{t+1} = \mu_1 + \phi_{1t} + a_{11}\chi_t, \tag{28}$$

$$\chi_{t+1} = \mu_2 + \phi_{2t} + a_{21}\chi_t + a_{22}\chi_{t-1}, \tag{29}$$

$$\chi_{t+1} = \mu_3 + \phi_{3t} + a_{31}\chi_t + a_{32}\chi_{t-1} + a_{33}\chi_{t-2}, \tag{30}$$

respectively, were determined for each time series. The expected value of a_{11} for the vegetation series in region A is given by the slope of the Beverton and Holt (1957) model at its positive equilibrium. Similarly, in region B the Cayley-Hamilton theorem gives that the expected values for a_{21} and a_{22} of the vegetation- and the herbivore-series are determined up to their sign by the coefficients of characteristic equation of (8), cf Akaike (1974). This argument applies for region C, too, so that a_{31}, a_{32}, and a_{33} are determinable through the coefficients of the characteristic equation of (16). The noise assumed for the autoregressive models are given by ϕ_{it}, i=1,2,3. We remark that this noise is not a dynamical quantity like the noise added in (27) in the beginning of this section; it describes the distance from the models (28)-(30) to the data generated by (27).

In Figure 3(b)-(d) the results are shown for the vegetation series (b), the herbivore series (c), and the carnivore series (d). In region A dark dots represent a_{11} for the vegetation series and the values expected from the Beverton and Holt (1957) model are denoted with solid line. In regions B and I, dark dots represent the obtained values of a_{21} whereas grey dots represent the obtained values of a_{22} for the vegetation- and the herbivore-series. The corresponding values determined by the characteristic equation of (8) are denoted with a solid and a dashed line, respectively. In regions C-H, dark dots and grey dots represent a_{31} and a_{32}, respectively, and light dots represent a_{33} for all time series. Solid, dashed, and dashdotted lines represent the corresponding values calculated from the characteristic equation at $(\hat{X}, \hat{U}, \hat{Z})$. In vast parts of regions D-H (12) was invalid and (16) was modified accordingly. The numbers given in Figures 3(b)-(d) represent the mean dimension estimates according to the AIC_C criterion, a variant of the Akaike (1973) information criterion, which includes correction terms for small sample sizes (Hurvich and Tsai (1989)).

Now consider the values for the coefficients obtained for the vegetation time-series, Figure 3(b). In region A they agree greatly with those predicted by the Beverton and Holt (1957)-model and the AIC_C-estimated dimension equals one as long as these predictions remain sufficiently different from zero. However, many of these coefficients are close to zero at the end of this region and the mean dimension equals zero. In region B these values do not agree with the values estimated by the Cayley-Hamilton theorem and (8). It seems like the autoregressive modeling approach tend to mix the two-dimensional dynamics with the one-dimensional Beverton-Holt dynamics. This is to a large extent confirmed by the AIC_C estimated dimension for the time series

which equals zero in this region because both coefficients remain as close to zero as the single coefficient was at the end of region A.

If we consider the herbivore time series, Figure 3(c) in region B, we observe that the coefficients a_{21} and a_{22} agree better with those predicted by the Cayley-Hamilton theorem and (8). We think that this is due to the fact that there is no single species model which is as close to the herbivore dynamics as was the case with the vegetation time-series. In this case a_{22} is predicted close to zero and remain so. Consequently, the AIC_C-criterion tries to neglect this additional coefficient and estimates the dimension of the herbivore-series to one for most parameter values.

We continue with region C. Here the expected values should agree with those predicted by the Cayley-Hamilton theorem and (16). From Figures 3(b)-(d) we deduce that this pattern is most valid for the carnivore series, since the fitting procedure again tends to mix the three level trophic interaction with two level trophic interactions and simple competition processes when herbivore and vegetation series are considered, respectively. The mean value of the dimension estimates for the vegetation series remains zero because a_{31} is not different enough from zero. A similar pattern dominates the herbivore series but here a_{32} becomes sufficiently different from zero at the end of the region, thus giving rise to the mean AIC_C dimension two. For the carnivore series both a_{31} and a_{32} are sufficiently different from zero throughout the interval and the AIC_C dimension equals two throughout the interval.

This pattern is continued in region D which describes carnivore-herbivore oscillations, but in such nonlinear regions neither Jacobians nor the Cayley-Hamilton theorem gives predictions of what is expected to occur. The AIC_C-dimension of the vegetation series equals zero in the beginning of the interval and increases so that it reaches two in the middle of the interval and this dimension is kept because a_{33} remains too close to zero to be taken into account. The AIC_C-dimension of the herbivore series remains two almost throughout the interval but starts approaching three at the end of the interval. The AIC_C-dimension of the carnivore series approaches the value three already in the beginning of the interval and several values higher than three were observed at the end of the interval.

For the rest of the parameter space with oscillating dynamics quite high dimensional models were considered as the most appropriate ones according to the AIC_C-criterion. But the variation is large here. Usually more lags were required for describing higher trophic levels and this was the pattern

already observed when fixed point dynamics in region C were considered. For instance, in regions E and F most vegetation series were described properly with respect to the AIC_C-criterion with two lags whereas most carnivore series required four lags. Usually the herbivore series required three lags but a large variation was present. In regions G and H the number of lags required for a description of the series varies from 2-7 for the vegetation series, from 3-6 for the herbivore series, and from 3-7 for the carnivore series. All types of series possessed roughly the same mean values for the number of required lags. In region I only vegetation- and herbivore series were available and their AIC_C-dimensions varied around six. We had the impression that the highest dimensional linear models were fitted when an almost periodic orbit was under consideration. This observation was clearest when low noise-levels were appended to (27).

The coefficients marked for the fitted models (28)-(30) in Figures 3(b)-(d) only occasionally described non-stationary models. A few cases were noted for the carnivore series in the end of region H and we denoted them by x-marks. When noise is added to the model it will give rise to sustained oscillations with roughly the same periods as those found in the original time-series (Akaike (1969)). Further evidence of this fact is given by the observation that the values obtained for the coefficients agree roughly with those obtained for empirical time-series with periods in the vicinity of ten, cf. Stenseth et. al. (1997).

The above coefficients have often been given interpretations in terms of direct- and delayed density dependence (Stenseth et. al. (1996)[48]) and in some cases they have been interpreted in terms of self-regulation and trophic interaction, (Stenseth et. al. (1996)[47]). Such interpretations have a clear connection to fundamental ideas in ecological literature, cf. May (1974) and Varley, Gradwell, and Hassell (1973). However, one should keep in mind that the relationship between delayed density dependence and population regulation is not simple, cf. Murdoch and Walde (1986) and Lindström (1999). Another complicated relationship remains between delayed density dependence and oscillation generating mechanisms. Note finally concerning our analysis that in no single case has intraspecific competition been assumed at other trophic levels than at the vegetation level and in no single case any observed oscillations have been caused by intraspecific competition.

Attempts to interpret the optimal number of lags can be found in the literature, too, and one of them interprets it as the "number of trophic levels influencing the species under consideration" (Stenseth et. al. (1997)). In

this way they conjecture that the snowshoe hare in boreal forests of North America is regulated from above and below whereas the Canadian lynx is primarily influenced by the snowshoe hare. In this section we used the AIC_C-criterion to determine the optimal number of lags but found no evidence for that the number of trophic levels taking part in the interaction could be predicted in such a way. Instead, we found a number of other (geometric) quantities affecting these dimension measures. We think that this holds for other automatic selectors of the smoothing parameters as well. In particular, we verify this conjecture for the generalized cross-validation criterion (GCV) in Section 6.

6 Nonparametric modeling of the food-chain

One characteristic feature of the deterministic dynamics of our model (2) is the presence of stable periodic orbits and chaos. These patterns cannot be recovered using AR-models fitted to data generated by (27), cf. Tong (1990). In this section we check into what extent and to what costs these patterns can be recovered using MARS (multivariate adaptive regression splines), a non-parametric modeling approach suggested by Friedman (1991). It has also been applied to one-observable time-series data, cf Lewis and Stevens (1991) and Lewis and Ray (1997). Their adaptations of MARS follow the guidelines given by Takens (1981) who concluded that lagged variables can be used as surrogates for unknown quantities.

If a general smooth model allowing interaction between all lags is fitted to data generated by a smooth dissipative model, then a sufficient number of lags is twice the number of variables included in the original smooth model, cf. Sauer, Yorke, and Casdagli (1991). The (lower) box-counting dimension is used for strange attractors in this context. We shall refer to this estimate as the 2D-estimate for further reference. It holds as long as a fully deterministic non-transient time-series is used and properties inside the attractor are predicted. It is of importance to note that positive and negative Lyapunov exponents are associated with properties inside and outside the attractor, respectively.

In our case several of the above assertions are violated. The model (2) is not smooth though its close relative (1) is smooth. In the deterministic case (2) possesses a number of parameter values corresponding to negative Lyapunov exponents, cf. Figure 1(b). We hope that these patterns can be

captured using model (27). We added noise to the models in Section 5, too, and the idea behind this procedure was to supply information regarding the map outside the attractor. We shall also focus on what can be predicted using continuous non-smooth additive models. Additive models have been preferred because biological data are usually expensive and short time-series are governing. The question concerning non-additivity should be set: To what extent is it to be detected from our time-series and how much data is needed for that. Non-smooth models were preferred because in terms of accuracy, no gain is received if smoothness is required (Friedman (1991)). We shall also experience that properties associated with the first partial derivatives of the map, like Lyapunov exponents are not predicted correctly anyway.

MARS models of fours types were fitted to each time series, the one-dimensional autoregressive model (28), a general linear model, a general additive model, and a non-additive model allowing interaction between two lags. MARS requires some upper limit for the number of lags to be included in the model and a 2D-estimate was calculated from the number of species taking part in the interaction. Since most of the assertions for this estimate were violated, it was corrected upwards so that the AIC_C-dimension calculated in Section 5 was used when higher. Then the deterministic versions of the fitted additive MARS-models were iterated and analyzed numerically as we did with the map (2) in Section 4.

The results are shown in Figures 4-6. Figure 4 shows the results for the vegetation-series. In Figure 4(a) we plotted three different amplitudes. A solid line denotes the amplitude for the vegetation series as predicted by (2). As small amount of noise was added and (27) predicts the amplitude indicated by the light dots. Finally, as the deterministic MARS-model was iterated, the amplitude corresponding to the circles was predicted. Some of the fitted MARS-models predicted diverging solutions and the density of these models are indicated with black dots above the letters indicating the dynamic region of the map (2).

Similarly, we have indicated the periods and the dominating periods in the Figures 4(b)-(c). In general, the dominating periods are predicted at least as well as the amplitude. The period-diagram in Figure 4(b) shows why measuring Lyapunov exponents for the MARS-models would be unnecessary. In several cases the fitted MARS model predicts a periodic solution when a deterministically chaotic or quasiperiodic was what was obtained using (2). The problem is present also in the converse direction; the fitting procedure

might destabilize periodic attractors obtained by (2). Our investigation indicated that this phenomenon was extremely robust ie it did not disappear by adding smoothness to neither generating maps nor fitted models. The presence of diverging solutions indicated by the density-plot in Figure 4(a) were strongly related to this phenomenon.

Figure 4(d) shows the GCV-estimates for the different types of models fitted to the time-series. The higher solid line shows the GCV for (28). Similarly, the higher dotted line gives the GCV for a general linear model. The mean of the number of lags used in this linear model for each dynamical region is given by a number in this figure. Comparing these dimension estimates with those obtained by AIC_C in Figure 3(b) shows that the optimal model according to GCV generally has higher dimension than that obtained by AIC_C. We see that (28) works well in terms of GCV throughout regions *A*, *B*, and for large parts of *C*. The lower solid line in Figure 4(d) gives the GCV for the additive model and the mean number of lags used in this model is given by the numbers in Figure 4(b). A comparison between the numbers given in Figures 4(b) and (d) shows that an additive model has a higher capacity to detect lags than the linear model. The lower dotted line in Figure 4(d) gives the GCV for a non-additive model allowing interaction between two lags. With 256 data-points a non-additive model is not much better than the additive except for possibly in regions *H* and *I*. A linear model works surprisingly well not only in regions *A*-*C* but also in region *D*.

We analyzed the herbivore and the carnivore series as we did with the vegetation series above and plotted the results in Figures 5-6. About 60-80% of the models fitted to the herbivore series generated diverging solutions in regions *E*-*G*, cf. our density plot in the upper part of Figure 5(b). The amplitudes of the rest of the fitted models did in general not correspond to those predicted by (2) and (27). From Figure 5(d) we see that (28) ceases to be an appropriate model outside region *B*. A general linear model works well throughout regions *B* and *C* and for some of the parameter values in region *D*. MARS detects clearly non-additivity in regions *E*-*G* but our tests with non-additive models fitted to data in these regions possessed diverging solutions as often as the fitted additive models.

Models fitted to the carnivore series possessed fewer diverging solutions than the models fitted to the vegetation and herbivore series. This result was evident for several regions, cf. the density plot in the top of Figure 6(a). The solutions of (2) and (27) were most different in region *H*, cf. the light dots and the solid line in Figure 6(a) and (c). Nevertheless, the deterministic MARS-

models fitted to (27) have a tendency to recover the deterministic dynamics of (2) as long as amplitudes and dominating periods only are analyzed. From Figure 6(d) we see that non-additive models were just slightly better in terms of GCV than the additive ones at the 256 data point level for the carnivore series.

7 Summary

In this paper we have derived and analyzed qualitatively a discrete model for a food-chain. Our qualitative analysis divides the parameter space roughly into nine different regions with respect to carrying capacity: persistence of the lowest trophic level (A), stable coexistence of vegetation and herbivores (B), stable coexistence of all three species possible (C), carnivore-herbivore oscillations (D), carnivore-herbivore oscillations interacting with stable herbivore-vegetation dynamics (E), increasing low-frequency carnivore-herbivore oscillations interacting with high-frequency herbivore-vegetation oscillations (F), decreasing carnivore-herbivore oscillations (G), herbivore-vegetation oscillations with co-oscillating carnivores (H), and pure herbivore-vegetation oscillations (I). Our analysis confirms an assertion by Gragnani et. al. (1998) which states that the mean carnivore-density is expected to have a local maximum at the boundary of chaos but shows also how violations of this principle may arise.

We were unable to detect cases where an invading carnivore can stabilize an oscillating herbivore-vegetation system and conjecture this to be true for (2). This stays in contrast to the stabilizing pattern found in continuous food-chains, cf. Freedman and Waltman (1977) and Oksanen et. al. (1981). This might be due to a stabilizing property of unsaturated carnivores which is absent in discrete systems.

The above division of the parameter-space has the advantage that we know what trophic level and mechanism stay behind the observations. In region D the oscillations are caused by carnivores. In region E carnivores cause possible chaos and oscillations. In regions F-G the oscillations can be caused by either herbivores or carnivores but possible chaos is caused by the carnivores. The same holds for possible low-frequency behavior in addition to high-frequency behavior. In region H carnivores exist but their impact on the observed dynamics is negligible; the observed oscillations can be described through herbivore-vegetation interaction. In region I all observed oscillations

are caused by herbivores. Behind region I also herbivore induced chaos may occur.

We expect that these patterns can be captured using of statistical methods when long time-series of all species are simultaneously available, see e. g. Ives and Jansen (1998). Most difficulties should occur when distinguishing regions D and H. In both cases the system have persistent carnivore-populations and no low-frequency behavior indicating the impact of carnivores can be detected. The system possesses also periods of approximately the same frequency in both regions. These two cases respond, however, very differently to both carnivore-removal and enrichment. In region D the dynamics become more unpredictable through enrichment and stable through carnivore-removal. In region H enrichment will eliminate the carnivores and carnivore-removal will not change the dynamics significantly.

In many cases long simultaneous time-series of all involved species and age-classes do not exist. The question is then whether possibilities for detecting the above patterns using time-series methods based on one-observables remain. A number of attempts for doing this have been suggested and we verified that use of autoregression coefficients leaves only limited possibilities for creation of a working method.

We continued by checking what was predicted by fitted non-linear statistical models (MARS). The result was that usually amplitudes and dominating periods are predicted quite well but larger errors than those introduced by the noise added to the model were visible. In several regions MARS showed some tendency to recover the deterministic dynamics of the original model despite the added noise. The cost of using non-linear models was that we had in general no control over when a diverging solution was predicted. This problem was only occasionally present for the autoregressive (linear) approach. The presence of diverging solutions was related to the failure to predict periods and Lyapunov exponents correctly and the fitting procedure both stabilized and destabilized attractors as was the case with noise added to models, cf. Rand and Wilson (1991). It is interesting to note that attempts to repair the divergence problems exist in contexts where the purpose is the determination of the Lyapunov exponent from time-series data, cf Turchin and Taylor (1992).

The different types of models were compared with respect to their GCV-values, an automatic smoothing parameter selection criterion possessing a potential to handle outliers, cf. Green and Silverman (1994). Despite the presence of non-additive data in all regions except A, non-additivity was de-

tected at the 256 data points level in a few cases only. In some of these cases a high number of models possessing diverging solutions were observed when fitted to the herbivore series but the use of non-additive models did not provide a solution to this problem. Our amounts of data and the added amount of noise were in general large enough to reject linear models in terms of GCV outside regions *A-D*. Region *D* possessed deterministic oscillations and fitting linear models here gives rise to false conclusions about the underlying reason for the oscillations. In addition, statistical methods have been applied to data-sets much shorter than the data-sets analyzed in this work and we are afraid of a large underlying potential for oversimplification when biological data is analyzed statistically.

Acknowledgments This paper was written as a part of a community training project financed by the European Commission through the Training and Mobility of Researchers (TMR) Programme and has received support from The Research Council of Norway (Programme for Supercomputing) through a grant of computer time.

References

[1] H. Akaike. Power spectrum estimation through autoregressive model fitting. *Annals of the Institute of Statistical Mathematics*, 21:407–419, 1969.

[2] H. Akaike. Information theory and an extension of the maximum likelihood principle. In B. N. Petrov and F. Csaki, editors, *2nd International Symposium on Information Theory*, pages 267–281. Akademia Kiado, Budapest, 1973.

[3] H. Akaike. Markovian representation of stochastic processes and its application to the analysis of autoregressive moving average processes. *Annals of the Institute of Statistical Mathematics*, 26:363–387, 1974.

[4] D. G. Aronson, M. A. Chory, G. R. Hall, and R. P. McGehee. Bifurcations from an invariant circle for two-parameter families of maps of the plane: A computer-assisted study. *Communications in Mathematical Physics*, 83:303–354, 1982.

[5] J. R. Beddington and P. S. Hammond. On the dynamics of host-parasite-hyperparasite interactions. *Journal of Animal Ecology*, 46:811–821, 1977.

[6] R. J. H. Beverton and S. J. Holt. *On the Dynamics of Exploited Fish Populations*, volume 19 of *Fisheries Investigation Series 2.* Ministry of Agriculture, Fisheries and Food, London, 1957.

[7] D. J. Borror, D. M. DeLong, and C. A. Triplehorn. *An Introduction to the Study of Insects.* Holt, Rinehart, and Winston, fourth edition, 1976.

[8] C.-H. Chiu and S.-B. Hsu. Extinction of top-predator in a three-level food-chain model. *Journal of Mathematical Biology*, 37:372–380, 1998.

[9] A. Cohn. Über die Anzahl der Wurzeln einer algebraischen Gleichung in einem Kreise. *Matematische Zeitschrift*, 14:110–148, 1922.

[10] L. C. Cole. The population consequences of life history phenomena. *The Quarterly Review of Biology*, 29:103–137, 1954.

[11] J. M. Cushing, B. Dennis, R. A. Desharnais, and R. F. Costantino. An interdisciplinary approach to understanding nonlinear ecological dynamics. *Ecological Modelling*, 92:111–119, 1996.

[12] H. I. Freedman and P. Waltman. Mathematical analysis of some three-species food-chain models. *Mathematical Biosciences*, 33:257–276, 1977.

[13] J. H. Friedman. Multivariate adaptive regression splines. *The Annals of Statistics*, 19(1):1–141, 1991.

[14] A. Gragnani, O. De Feo, and S. Rinaldi. Food chains in the chemostat: Relationships between mean yield and complex dynamics. *Bulletin of Mathematical Biology*, 60:703–719, 1998.

[15] P. J. Green and B. W. Silverman. *Nonparametric regression and Generalized Linear Models*, volume 58 of *Monographs on Statistics and Applied Probability.* Chapman & Hall, 1994.

[16] M. Gyllenberg, I. Hanski, and T. Lindström. A predator-prey model with optimal suppression of reproduction in the prey. *Mathematical Biosciences*, 134:119–152, 1996.

[17] M. Gyllenberg, I. Hanski, and T. Lindström. Continuous versus discrete single species population models with adjustable reproductive strategies. *Bulletin of Mathematical Biology*, 59(4):679–705, 1997.

[18] M. P. Hassell, J. H. Lawton, and R. M. May. Patterns of dynamical behaviour in single-species populations. *Journal of Animal Ecology*, 45:471–486, 1976.

[19] A. Hastings and T. Powell. Chaos in a three-species food chain. *Ecology*, 72(3):896–903, 1991.

[20] C. M. Hurvich and C.-L. Tsai. Regression and time series model selection in small samples. *Biometrika*, 76:297–307, 1989.

[21] A. R. Ives and V. A. A. Jansen. Complex dynamics in stochastic tritrophic models. *Ecology*, 79:1039–1052, 1998.

[22] E. I. Jury. *Theory and application of the z-transform method.* John Wiley & Sons, Inc, 1964.

[23] A. Klebanoff and A. Hastings. Chaos in three species food chains. *Journal of Mathematical Biology*, 32:427–451, 1994.

[24] Y. Kuang and H. I. Freedman. Uniqueness of limit cycles in Gause-type models of predator-prey systems. *Mathematical Biosciences*, 88:67–84, 1988.

[25] P. A. W. Lewis and B. K. Ray. Modeling long-range dependence, nonlinearity, and periodic phenomena in sea surface temperatures using TSMARS. *Journal of the American Statistical Association*, 92(439):881–893, 1997.

[26] P. A. W. Lewis and J. G. Stevens. Nonlinear modeling of time series using multivariate adaptive regression splines (MARS). *Journal of the American Statistical Association*, 86(416):864–877, 1991.

[27] T. Lindström. Dependencies between competition and predation - and their consequences for initial value sensitivity. *SIAM Journal of Applied Mathematics*, 1999. To appear.

[28] A. Łomnicki. *Population Ecology of Individuals*, volume 25 of *Monographs in Population Biology*. Princeton University Press, Princeton, New Jersey, 1988.

[29] A. J. Lotka. *Elements of Physical Biology*. Williams and Wilkins, Baltimore, 1925.

[30] M. Marden. *Geometry of polynomials*. Providence, R. I.: American Mathematical Society, 1966.

[31] R. M. May. Stability in multispecies community models. *Mathematical Biosciences*, 12:59–79, 1971.

[32] R. M. May. On relationships among various types of population models. *The American Naturalist*, 107(953):46–57, 1973.

[33] R. M. May. *Stability and Complexity in Model Ecosystems*. Princeton University Press, Princeton, second edition, 1974.

[34] J. A. J. Metz and O. Diekmann. *The Dynamics of Physiologically Structured Populations*. Springer-Verlag, 1986.

[35] W. F. Morris. Problems in detecting chaotic behavior in natural populations by fitting simple discrete models. *Ecology*, 71(5):1849–1862, 1990.

[36] W. W. Murdoch and S. J. Walde. Analysis of insect population dynamics. In P. J. Grubb and J. B. Whittaker, editors, *Toward a more exact ecology*, pages 113–140. Blackwell, 1989.

[37] A. J. Nicholson and V. A. Bailey. The balance of animal populations. - Part I. In *Zool. Soc. (London), Proc. 3*, pages 551–598, 1935.

[38] R. Nisbet, S. Blythe, B. Gurney, H. Metz, and K. Stokes. Avoiding chaos. *Trends in Ecology and Evolution*, 4(8):238–240, 1989.

[39] L. Oksanen, S. D. Fretwell, J. Arruda, and P. Niemelä. Exploitation ecosystems in gradients of primary productivity. *The American Naturalist*, 118(2):240–261, 1981.

[40] S. L. Pimm. *Food Webs*. Chapman and Hall, London, New York, 1982.

[41] S. L. Pimm and J. H. Lawton. Number of trophic levels in ecological communities. *Nature*, 268:329–331, 1977.

[42] D. A. Rand and H. B. Wilson. Chaotic stochasticity: a ubiquitous source of unpredictability in epidemics. *Proceedings of the Royal Society of London B*, 246:179–184, 1991.

[43] M. L. Rosenzweig. Exploitation in three throphic levels. *The American Naturalist*, 107(954):275–294, 1973.

[44] T. Sauer, J. A. Yorke, and M. Casdagli. Embedology. *Journal of Statistical Physics*, 65:579–616, 1991.

[45] J. Schur. Über Potenzreihen, die im Innern des Einheitskreises beschränkt sind. *Journal für die reine und angewandte Mathematik*, 147:205–232, 1917.

[46] J. Schur. Über Potenzreihen, die im Innern des Einheitskreises beschränkt sind. *Journal für die reine und angewandte Mathematik*, 148:122–145, 1918.

[47] N. C. Stenseth, O. N. Bjørnstad, and W. Falck. Is spacing behaviour coupled with predation causing the microtine density cycle? A synthesis of current process-oriented and pattern-oriented studies. *Proceedings of the Royal Society of London B*, 263:1423–1435, 1996.

[48] N. C. Stenseth, O. N. Bjørnstad, and T. Saitoh. A gradient from stable to cyclic populations of *Clethrionomys rufocanus* in Hokkaido, Japan. *Proceedings of the Royal Society of London B*, 263:1117–1126, 1996.

[49] N. C. Stenseth, W. Falck, O. Bjørnstad, and C. J. Krebs. Population regulation in snowshoe hare and Canadian lynx: Asymmetric food web configurations between hare and lynx. *Proceedings of the National Academy of Sciences of the United States of America*, 94:5147–5152, 1997.

[50] G. Sugihara and R. M. May. Nonlinear forecasting as a way of distinguishing chaos from measurement error in time series. *Nature*, 344:734–741, 1990.

[51] F. Takens. Detecting strange attractors in turbulence. In D. A. Rand and L. S. Young, editors, *Dynamical Systems and Turbulence, Warwick 1980, Lecture Notes in Mathematics 898*, pages 366–381. Springer-Verlag, 1981.

[52] H. Tong. *Non-linear Time Series.* Clarendon Press, 1990.

[53] P. Turchin. Nonlinear time-series modeling of vole population fluctuations. *Researches on Population Ecology*, 38(2):121–132, 1996.

[54] P. Turchin and A. D. Taylor. Complex dynamics in ecological time series. *Ecology*, 73(1):289–305, 1992.

[55] G. C. Varley, G. R. Gradwell, and M. P. Hassell. *Insect Population Ecology.* Blackwell, 1973.

[56] K. Vibe and J.-M. Vesin. On chaos detection methods. *International Journal of Bifurcation and Chaos*, 6(3):529–543, 1996.

[57] V. Volterra. Variazioni e fluttuazioni del numero d'individui in specie animali conviventi. *Memorie della R. Accademia Nationale dei Lincei 6*, 2:31–113, 1926.

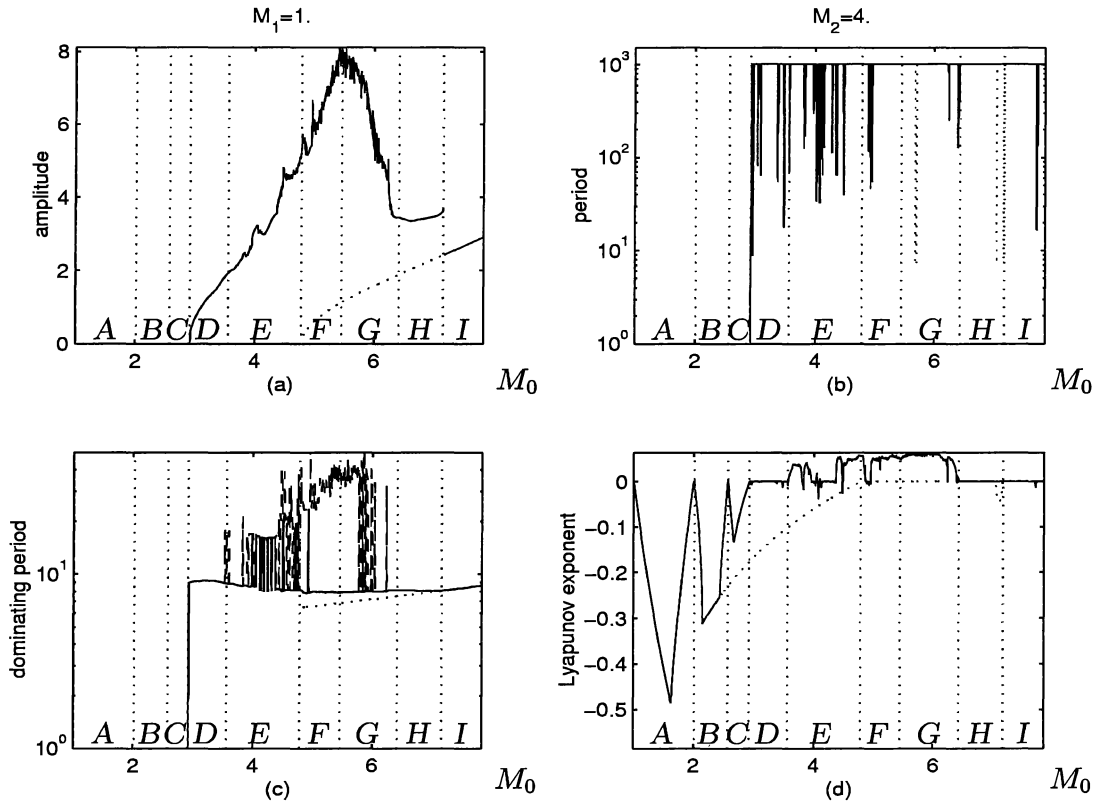

Figure 1: Deterministic dynamics of the approximative food-chain model (2) (solid line) and the corresponding two-dimensional model (6) (dotted line) in different regions of the parameter space separated by dotted lines. (a) amplitudes. (b) periods. (c) dominating periods calculated from vegetation (solid) and the carnivores (dashed). (d) Lyapunov exponents.

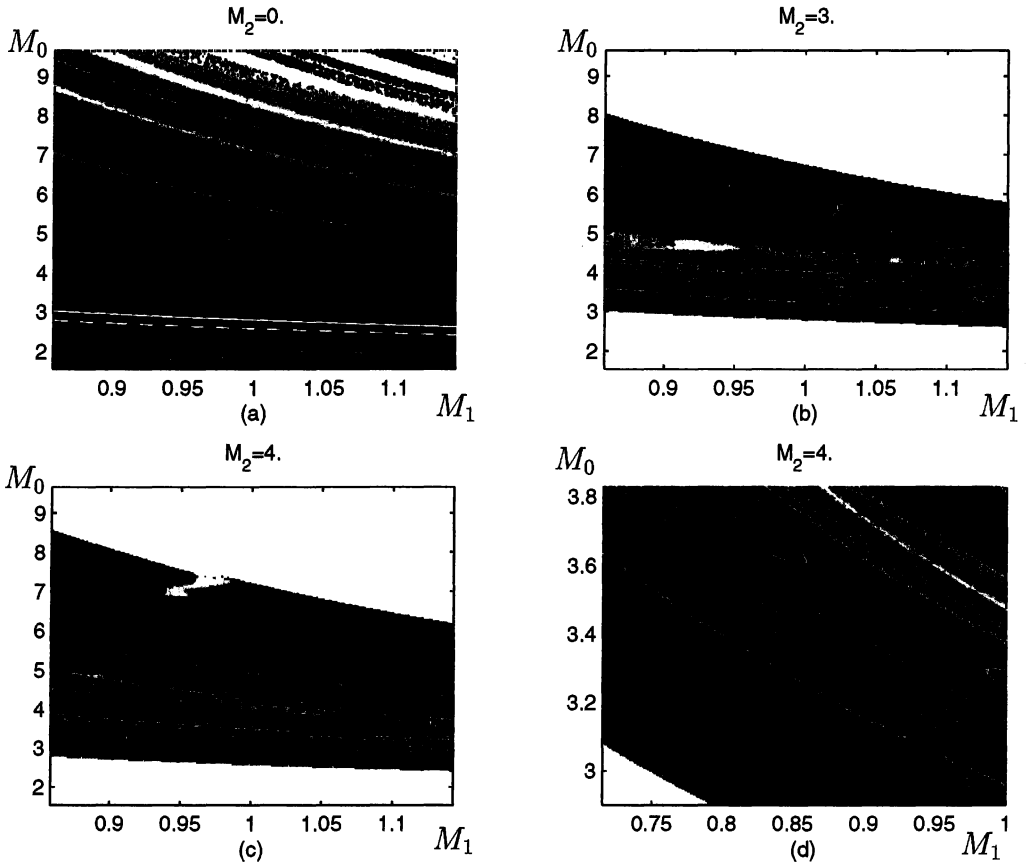

Figure 2: Deterministic dynamics of the approximative food-chain model (2). In (a) the dynamics of (6) is given in the (M_1, M_0)-plane as follows: Green dots represent dynamics governed by the fixed point $(M_0 - 1, 0, 0)$, black dots locally stable coexistence, yellow dots low-periodic solutions, light blue dots high-periodic solutions where no period below 1024 was found, blue dots quasiperiodic or bifurcating solutions, and finally red dots represent chaotic solutions. In (b) the region affected by carnivore invasion at $M_2 = 3.$ is plotted and the corresponding solutions are given as in (a). In (c) the region affected at $M_2 = 4.$ is given in the same way and (d) gives details of (c) close to the applicability range of Theorem 3.4.

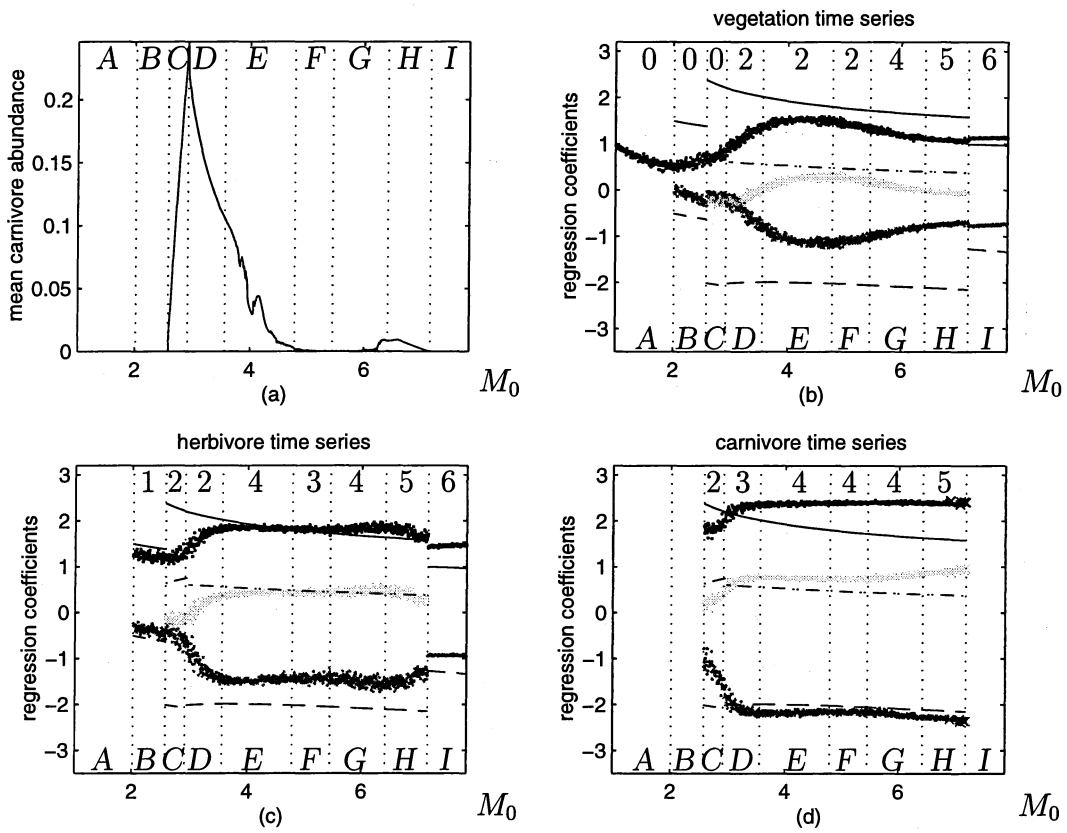

Figure 3: (a) The mean deterministic carnivore abundance has a local optimum at the boundary of chaos and high-frequency cycles. (b)-(d) Time series describing each trophic level has been generated by (27) and different regression coefficients are calculated for the log-transformed results. (b) Regression coefficients of the vegetation time series. (c) Regression coefficients of the herbivore time series. (d) Regression coefficients of the carnivore time series. The numbers indicate the mean AIC_C-dimension of the time-series in the corresponding region.

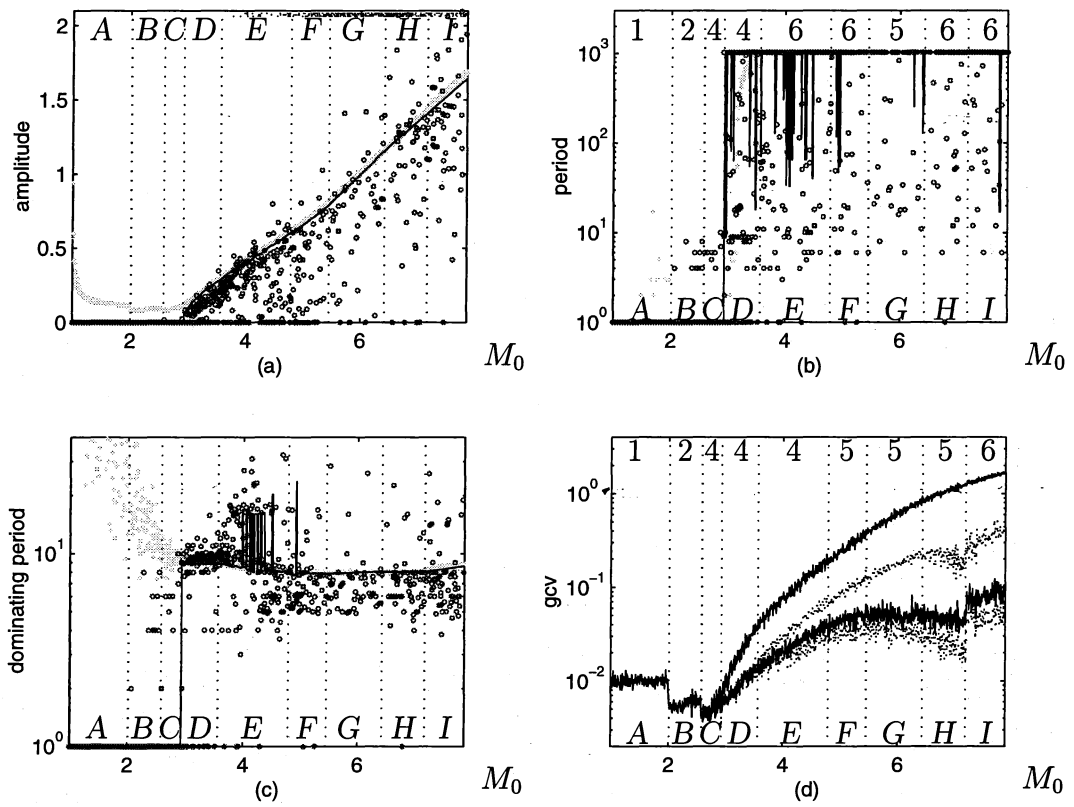

Figure 4: In (a)-(c) the deterministic predictions of (2) for the vegetation time-series are given by a solid line. A small amout of noise is added (cf. (27)) and the prediction given by grey dots is obtained. The corresponding prediction given by iteration of a fitted MARS-model is given by circles. A density-plot along the upper line of the diagram of (a) tells how many MARS-models predicted diverging solutions. (a) Amplitude. (b) Periods. The numbers indicate the mean dimension of the fitted additive models in each of the regions, A, B, etc. (c) Dominating periods. (d) From above: GCV for the best AR(1) model (solid), linear model (dotted), additive model (solid), non-additive model found by MARS (dotted). The numbers indicate the mean dimension of the fitted linear models in each of the regions, A, B, etc.

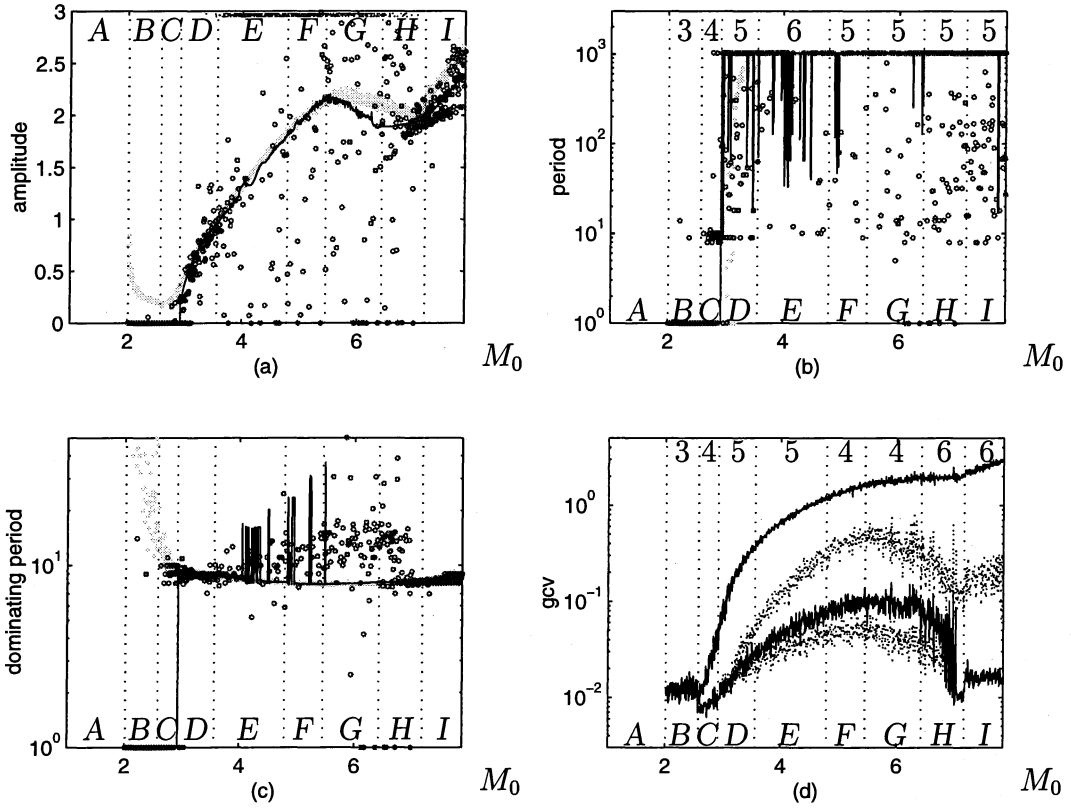

Figure 5: In (a)-(c) the deterministic predictions of (2) for the herbivore time-series are given by a solid line. A small amout of noise is added (cf. (27)) and the prediction given by grey dots is obtained. The corresponding prediction given by iteration of a fitted MARS-model is given by circles. A density-plot along the upper line of the diagram of (a) tells how many MARS-models predicted diverging solutions. (a) Amplitude. (b) Periods. The numbers indicate the mean dimension of the fitted additive models in each of the regions, B, C, etc. (c) Dominating periods. (d) From above: GCV for the best AR(1) model (solid), linear model (dotted), additive model (solid), non-additive model found by MARS (dotted). The numbers indicate the mean dimension of the fitted linear models in each of the regions, B, C, etc.

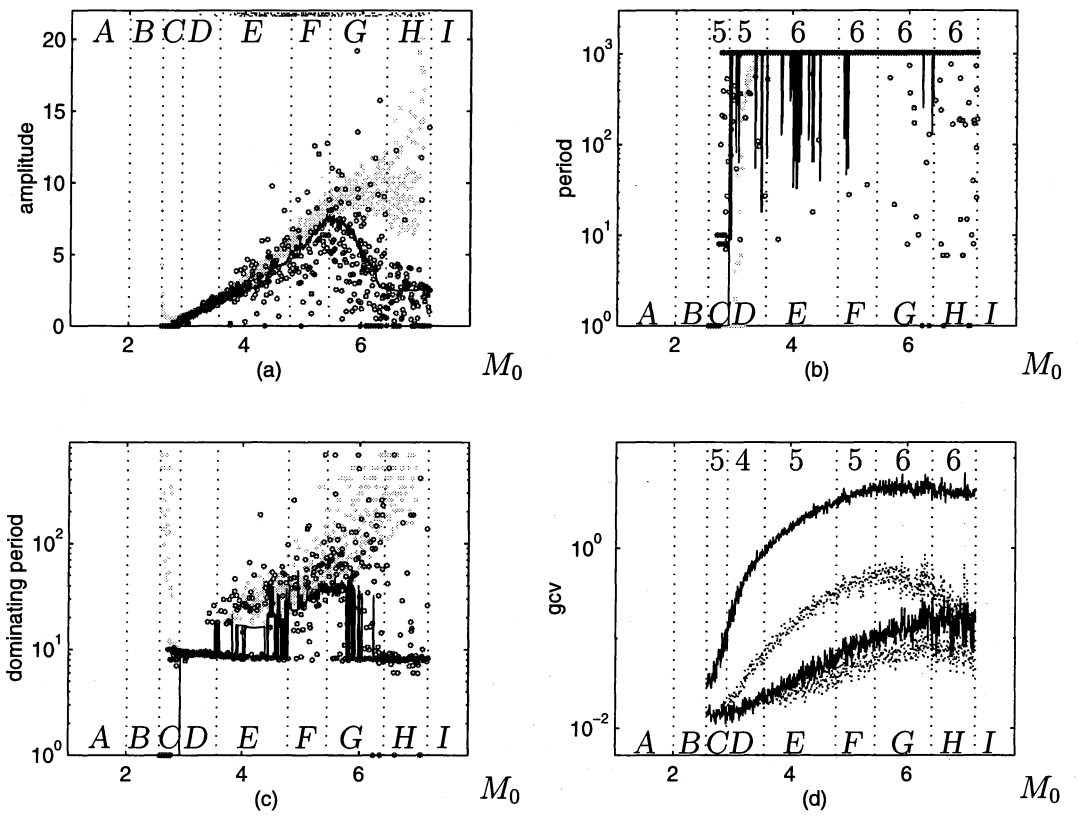

Figure 6: In (a)-(c) the deterministic predictions of (2) for the carnivore time-series are given by a solid line. A small amout of noise is added (cf. (27)) and the prediction given by grey dots is obtained. The corresponding prediction given by iteration of a fitted MARS-model is given by circles. A density-plot along the upper line of the diagram of (a) tells how many MARS-models predicted diverging solutions. (a) Amplitude. (b) Periods. The numbers indicate the mean dimension of the fitted additive models in each of the regions, C, D, etc. (c) Dominating periods. (d) From above: GCV for the best AR(1) model (solid), linear model (dotted), additive model (solid), non-additive model found by MARS (dotted). The numbers indicate the mean dimension of the fitted linear models in each of the regions, C, D, etc.